




Influence of bioactive peptides from fermented red lentil protein isolate on gut microbiota: A dynamic *in vitro* investigation

Federica Mastrolonardo^a, Stefano Tonini^b, Lena Granehall^a, Andrea Polo^{a,b}, Emanuele Zannini^{c,d}, Marco Gobetti^{a,b}, Raffaella Di Cagno^{a,b}, Olga Nikoloudaki^{a,b,*} 

^a Faculty of Agricultural, Environmental and Food Sciences, Free University of Bozen-Bolzano, Piazza Università 5, 39100, Bolzano, Italy

^b International Center on Food Fermentation, 39100 Bolzano, Italy

^c University College Cork, School of Food and Nutritional Sciences, College Road, Cork T12 K8AF, Ireland

^d University of Rome Sapienza, Department of Environmental Biology, Piazzale Aldo Moro 5, 00185, Roma, Italy

ARTICLE INFO

Keywords:

Fermentation
Protein digestibility
Legumes
Butyric acid
Sustainability
Plant-based ingredients
Gut microbial ecosystem

ABSTRACT

Lentils are recognized as sustainable alternative protein sources due to their favorable nutritional and functional profiles. This study evaluated the protein quality and digestibility of raw (RRLPI) and fermented (FRLPI) red lentil protein isolates and assessed their impact on the gut microbiota using the SHIME® *in vitro* dynamic gut model. Fermentation significantly increased *in vitro* protein digestibility (IVPD), from 92.5 % in RRLPI to 94.5 % in FRLPI ($p < 0.05$). Amino acid profiling revealed that while sulfur-containing amino acids decreased, threonine and other key essential amino acids were better preserved or enriched in FRLPI when expressed per gram of protein. Feeding with FRLPI promoted the growth of potentially beneficial colonic genera such as *Lactiplantibacillus* and *Furfurilactobacillus* and stimulated short-chain fatty acid (SCFA) production, with a notable increase in butyrate. Moreover, FRLPI digestion yielded a greater release of low-molecular-weight peptides (<3 kDa), some of which exhibited predicted antioxidant and ACE-inhibitory activities. Together, these results highlight fermentation as a strategy to optimize lentil protein functionality, improving gut microbial ecology, nutrient bioavailability, and the release of health-relevant peptides.

1. Introduction

Proteins are crucial macronutrients in the human diet and have essential biological functions (Baladrán-Quintana et al., 2019). To provide enough protein while minimizing environmental impact, the diet should include both plant and animal sources, with an emphasis on plant-based foods. In fact, the transition from animal to plant-based proteins is necessary to achieve a sustainable future (Boven et al., 2024; De Boer and Aiking et al., 2011). The production of plant-based foods is generally more sustainable when considering land and water use, energy conversion and greenhouse gas emissions, while proteins of animal origin tend to involve much of fresh water, land, and CO₂ (Lumsden et al., 2024). Moreover, the intensive breeding to increase

animal protein production is linked to emerging zoonotic diseases and antimicrobial resistance (Aiking et al., 2020). Not only are proteins of plant origin more environmentally friendly to produce, but the consumption of plant-based foods, compared to animal-based ones, could be associated with many health benefits (Bryant, 2022).

Pulses are considered promising plant protein sources due to their adaptability, low cost, and nutritional profile (Du et al., 2023). Red lentils, which make up 70 % of global lentil production (*Lens culinaris*), are rich in carbohydrates, proteins, fibers, vitamins, and minerals, and are appealing for meat substitutes due to their high protein, dietary fiber content, and low fat and cholesterol levels (Du et al., 2023; Roy et al., 2010; Lee et al., 2021). Moreover, consuming lentils provides numerous health benefits, including lowering the risk of metabolic syndrome,

Abbreviations: ANC, Antinutritional compounds; (ACE) inhibitory effects, Angiotensin-converting enzyme; BPs, Bioactive peptides; RLPI, Red lentil protein isolates; RRLPI, Raw red lentil protein isolate; FRLPI, Fermented red lentil protein isolate; SHIME, Simulator of the Human Intestinal Microbial Ecosystem; SDA, Saburou Dextrose Agar; DY, Dough yield; AAs, Amino acids; EAAs, Essential amino acids; NEAAs, Nonessential amino acids; IVPD, *In vitro* protein digestibility; PDCAAS, Protein digestibility-corrected amino acid score; ST/SI, Stomach and small intestine; PC, Proximal colon; DC, Distal colon; SCFAs, Short chain fatty acids; NIST, National Institute of Standards and Technology.

* Corresponding author at: Faculty of Agricultural, Environmental and Food Sciences, Free University of Bozen-Bolzano, Piazza Università 5, 39100, Bolzano, Italy.

E-mail address: olga.nikoloudaki@unibz.it (O. Nikoloudaki).

<https://doi.org/10.1016/j.fufo.2025.100772>

Received 7 February 2025; Received in revised form 29 July 2025; Accepted 23 September 2025

Available online 24 September 2025

2666-8335/© 2025 The Authors. Published by Elsevier B.V. This is an open access article under the CC BY license (<http://creativecommons.org/licenses/by/4.0/>).

helping prevent heart disease, and boosting antioxidant activity (Dhull et al., 2023). However, the exploitation of lentils is still limited by the presence of allergens and antinutritional compounds (ANCs) such as phytic acid, protease inhibitors, tannins, and lectins. Protease inhibitors (e.g., trypsin and chymotrypsin inhibitors) can significantly reduce protein digestibility if not removed or inactivated. The presence of phytates and oxalic acid can impair the bioavailability and digestibility of nutrients (Joehnke et al., 2021).

Lentil protein isolates (LPI) have gained increasing attention in recent years because they offer improved nutritional, functional, and sensory properties compared to whole lentil flour (Aghababaei et al., 2024). Modern extraction and processing methods enhance the nutritional profile of lentils by significantly reducing trypsin inhibitor activity, with reductions of up to 87 %. Furthermore, LPI contain substantially lower levels of galacto-oligosaccharides (GOS), which are important components of fermentable oligo-, di-, monosaccharides and polyols (FODMAPs). FODMAPs are fermentable short-chain carbohydrates that can cause digestive discomfort in individuals with irritable bowel syndrome (IBS). The reduction of galacto-oligosaccharides (GOS) in lentil protein isolates, ranging from 58 to 91 % compared to lentil flour, improves their potential tolerability and supports their inclusion in low FODMAP diets. The isolation process also improves protein digestibility by minimizing molecular interactions and complex formations, resulting in a more bioavailable and purified protein product that holds strong potential for human nutrition (Joehnke et al., 2021).

Fermentation is an effective, natural, and cost-efficient method to enhance nutrients bioavailability in pulses by degrading ANCs, thereby preventing food allergies and intolerances, and improving nutritional quality (Jeyakumar et al., 2022). Further, it allows the release (through hydrolysis by proteolytic enzymes) of bioactive peptides (BPs), which exert a plethora of bioactivities such as antioxidant, antimicrobial, antidiabetic, anti-inflammatory and ACE inhibitory activities (Sánchez et al., 2017). The biological effects of BPs depend on their structural properties, like chain length, amino acid composition and sequence, and their molecular mass (Chai et al., 2020; Tonini et al., 2024).

While diet is a primary determinant of gut microbiota composition, most studies focus on carbohydrates, leaving the impact of dietary protein and its derivatives less explored. This gap is most probably due to the difficulty in analyzing protein degradation in the colon. Undigested proteins reaching the colon can be fermented by gut bacteria, producing beneficial but also harmful microbial products like ammonia and amines, phenols, sulfides, and branched short-chain fatty acids, which, at high concentrations, can cause serious gastrointestinal disorders like inflammation and increase gut permeability, and should therefore be prevented (Guo et al., 2021). Conversely, selected high-quality proteins as dietary supplements can positively affect the host by optimizing the structure of gut microbiota, improving intestinal barrier function, and regulating the host's metabolic activities (Bao and Wu, J., 2021). Hence, the bioactive properties of proteins and peptides derived from lentils have gained increased recognition in food nutrition for their potential benefits in treating and reducing the onset of disease (Roy et al., 2010).

RLPI is a highly purified and concentrated source of high-quality protein, offering distinct advantages over traditional flour. Despite its potential benefits, the impact of RLPI on the gut microbiome and metabolome remains largely unexplored. We employed our optimized fermentation protocol (Tonini et al., 2024) to ferment RLPI, and investigate the interplay between protein digestibility of both fermented (FRLPI) and raw (RRLPI) RLPI, and the potential impact of the resulting BPs on colon ecosystems by using the Simulator of the Human Intestinal Microbial Ecosystem (SHIME®).

2. Material and methods

2.1. Raw ingredients and fermentation conditions

RLPI was chosen as one of the plant protein sources developed within the Smart Protein Project (EU Framework Program for Research and Innovation - Horizon 2020; <https://smartproteinproject.eu>). Produced via dry fractionation and supplied by Fraunhofer IVV (Freising, Germany), the RLPI was portioned and stored under vacuum conditions at room temperature until further use. *Hanseniaspora uvarum* SY1 from the culture collection of the Free University of Bozen-Bolzano (Italy) was used as a starter, which was kept in 20 % (v/v) glycerol stocks at -20°C and propagated twice in Sabouroud Dextrose Agar (SDA) broth for 24 h at 30°C (Tonini et al., 2024) prior inoculation. A fermentable liquid dough with a 500 dough yield ($\text{DY} = [\text{dough weight}/\text{flour weight}] \cdot 100$) was prepared by combining 3 kg of RLPI with 12 kg of water. The resulting mixture was fermented by *H. uvarum* SY1 and added glucose (1 %, w/w). The inoculum was done as previously described by Tonini et al. (2024). Briefly, after 24 h, cells were collected by centrifugation (10,000 rpm, 10 min at 4°C), washed twice in 50 mM sterile potassium phosphate buffer (pH 7.0), and then added to RLPI dough to a final cell density of approximately $5.0 \text{ Log CFU mL}^{-1}$. The fermentation was 8 days at 30°C in a Biostat®-CPlus bioreactor for semi-automated liquid-state fermentation (Sartorius AG, Germany). The RLPI without bacterial inoculum and not subjected to the fermentation was used as the control sample. Both samples underwent freeze-drying treatment (Lyostar II, FTS Kinetics, Stone Ridge, NY).

2.2. Amino acid profiling and protein digestibility assessment of substrates

Fermented RLPI (FRLPI) and raw RLPI (RRLPI) samples were subjected to three distinct hydrolysis methods to determine their amino acid (AA) profiles. Acid hydrolysis was performed following AOAC Method 994.12 for quantification of most amino acids, except cysteine (Cys), methionine (Met), and tryptophan (Trp). Sulfur-containing amino acids, Cys and Met, were quantified following performic acid oxidation (AOAC Method 994.12), while Trp was determined separately through alkaline sodium hydrolysis (AOAC Method 988.15). Amino acid analysis was conducted using a Biochrom 30 Series Amino Acid Analyzer (Biochrom Ltd., Cambridge Science Park, England) equipped with a sodium-cation exchange column ($20 \times 0.46 \text{ cm}$ internal diameter), as previously described by Di Cagno et al. (2017).

In vitro protein digestibility (IVPD) was evaluated using the Protein Digestibility Assay Kit (Megazyme International, Wicklow, Ireland) according to the manufacturer's instructions. The protein digestibility-corrected amino acid score (PDCAAS) was calculated by multiplying the amino acid score of the limiting essential amino acids (EAA) by the IVPD. The total protein content of the samples was determined using an NDA 702 Dumas Nitrogen Analyzer (VELP Scientifica, Italy).

2.3. SHIME® experiment

The experimental setup comprised two identical SHIME® lines operating in parallel. Each line included three double-jacketed bioreactors maintained at 37°C under anaerobic conditions, representing the stomach and small intestine (ST/SI), proximal colon (PC), and distal colon (DC), respectively, with continuous stirring (Koirala et al., 2022). Each bioreactor was flushed once daily with a sterile nitrogen (N_2) stream to prevent any presence of oxygen (O_2) (Molly et al., 1993). The PC and DC bioreactors were filled with 500 mL and 800 mL, respectively, of adult L-SHIME® PDNM001B growth medium (ProDigest, Gent, Belgium). The pH in the PC and DC ranged from 5.6 to 5.9 and from 6.6 to 6.9, respectively, and was computer-controlled using 0.5 M HCl and 0.5 M NaOH to mimic the physiological conditions of the colon. The ST/SI bioreactors were maintained at pH 2. Before starting, PC and DC bioreactors of both SHIME® lines were simultaneously inoculated with

5 % (v/v) of fresh fecal slurry from a selected and representative donor, as described by Da Ros et al. (2021). Fecal slurry was prepared before inoculation according to the method described by Molly et al. (1993). After inoculation, a static incubation of 12 h was first performed to allow initial microbiota adaptation. A stabilization period of 3 weeks followed, allowing the evolution of a stable colonic microbiota, followed by a 2-week control period representing the experimental baseline. During these 5 weeks, ST/SI bioreactors were fed three times a day (every 8 h) with the same amount of basal feed (of which protein ~2.06 g per day), consisting of 140 mL of pre-digested adult SHIME® feed PDNM001B (ProDigest, Gent, Belgium). In every feeding cycle, the feed resided 45-minute in the ST/SI bioreactor where 60 mL of pancreatic juice (12.5 g NaHCO₃, 6 g dehydrated bile extract and 0.9 g pancreatin (P1750, Merck, Italy) per L) were added. The content of ST/SI was finally transferred to the colon bioreactors. Subsequently, a 2-week treatment period started, during which the daily feeding (420 mL) was supplemented with FRLPI or RRLPI (one for each SHIME® line), provided in powder form, to a final concentration of 9 % (weight of powder/vol of feed). Specifically, the administered daily dose of RLPIs was about 37.8 g, for both RRLPI (approximately 31.37 g of proteins) and FRLPI (approximately 19.28 g of proteins). The difference in protein content between RRLPI and FRLPI is due to RRLPI consisting of 83 % protein on a dry weight basis, whereas FRLPI has a protein content of 51 % on a dry weight basis. Subsequently, a 1-week washout period followed. During this period, the bioreactors were fed with only basal feed, as during the stabilization and control periods. Throughout the simulation, lumen samples (40 mL) were collected from both PC and DC bioreactors at the end of control period (T0), after one week of treatment period (T1), after two weeks of treatment period (T2), and after one week of washout period (T3). Lumen samples were stored at –80 °C until further analysis.

2.4. Analysis of short chain fatty acids (SCFAs)

The SCFAs profile, namely acetate, propionate, and butyrate, was investigated on lumen samples from the SHIME® experiment. Extraction and analysis were conducted starting from two mL of sample, following the procedures described by Lotti et al. (2017). The extracts were injected into an Agilent 7890A gas chromatograph coupled to an Agilent 5975 quadrupole mass detector (Agilent Technologies Italia SpA, Cernusco sul Naviglio, Milano, Italy). For the chromatographic separation, a fused silica Stabilwax®- 42 DA column (30 m × 0.25 mm i.d. 0.25 mm) (Restek Corporation, Bellefonte, PA, USA) was used. Mass spectrometry detection was carried out in full-scan mode (electron ionization of 70 eV, an ion source temperature of 250 °C, *m/z* values ranging from 40 to 300 Da, and an acquisition scan time of 0.2 s). The identification of acetic, propionic, and butyric acids was achieved by comparing their mass spectra with those reported in the National Institute of Standards and Technology (NIST) US Government library.

2.5. Identification of low molecular weight peptides (LMWP)

Water soluble extracts (WSE) of fecal inoculum and lumen samples were prepared according to Tlais et al. (2022). LMWP were identified by Ultra-high-performance liquid chromatography high-resolution mass spectrometry (UHPLC/HR-MS2) (UHPLC Ultimate 3000, Thermo Scientific, San Jose, CA, USA; Q Exactive Hybrid Quadrupole-Orbitrap Mass Spectrometer, Thermo Scientific, San Jose, CA, USA) equipped with a C18 column (Acquity UPLC—C18 Reversed-phase, 2.1 × 100 mm, 1.8 µm particle size, Waters Corporation, Milford, MA, USA), as previously described by Martini et al. (2020). The MS data were processed using Proteome Discoverer 2.3 software (Thermo Fisher Scientific, Dreieich, Germany) with the Mascot search engine (Matrix Science, Boston, MA, USA) for peptide identification against the *Lens culinaris* peptidome database (<https://www.ncbi.nlm.nih.gov/protein/?term=tid3864>). The parameters used for the identification process were enzyme, no-enzyme, peptide mass tolerance, ± 5 ppm; fragment mass

43 tolerance, ±0.1 Da; variable modification, demethylation (NQ), oxidation (M) and phosphorylation (ST); the maximal number of post-translational modifications permitted in a single peptide was one. Peptides with sequences ranging from 4 to 30 AAs were analyzed. Only peptides identified with a significance threshold of *p* < 0.05 were included for further analysis. Identified peptides were screened for 100 % sequence homology with BPs reported in the literature using the BIOPEP-UWM database (Minkiewicz et al., 2019).

2.6. Microbiota composition

Seven milliliters of lumen samples were centrifuged at 10,000 rpm for 10 min at room temperature. Genomic DNA was extracted from the resulting pellet using the FastDNA Spin Kit for Soil (MP Biomedicals, Irvine, CA, USA) according to the manufacturer's instructions. Each sample was extracted in duplicate. DNA concentration was quantified using Nanodrop One/One Spectrophotometer (Thermo Fisher Scientific, San Jose, CA, USA). A total of 32 DNA extracts were sequenced. DNA metabarcoding library preparation and sequencing were carried out by AllGenetics & Biology SL (www.allgenetics.eu). For prokaryotic library preparation, the V4 (~420 bp) region of the 16S rRNA gene was amplified using the Bakt_341F and Bakt_805R primers (Herlemann et al., 2011) with Illumina sequencing primers attached at the 5' ends. The Polymerase Chain Reaction (PCR) was conducted in a 12.5 µL reaction volume with 1.25 µL of 1:10 diluted DNA template, 0.5 µM primers, 3.13 µL of Supreme NZYtaq 2x Green Master Mix (NZYTech), and ultrapure water. The PCR conditions included an initial denaturation at 95 °C for 5 min, 25 cycles of 95 °C for 30 s, 56 °C for 45 s, 72 °C for 45 s, and a final extension at 72 °C for 7 min. A second amplification step attached oligonucleotide indices for multiplexing with 5 cycles at 60 °C. Negative controls were included to check for contamination. Libraries were verified on 2 % agarose gels, purified using Mag-Bind RXNPure Plus magnetic beads (Omega Biotek), and pooled in equimolar amounts based on Qubit quantification. Sequencing was performed using a MiSeq PE300 flow cell (Illumina) in two runs due to insufficient initial yield. Paired-end sequences were subjected to quality control, merging, and chimera removal via DADA2 v1.24.0 (Callahan et al., 2016). Taxonomic classification to the genus level was performed using DADA2's RDP naive Bayesian classifier method and the Silva v138.1 database.

2.7. Statistical and multivariate data analysis approaches

Analyses of protein digestibility, and AAs profiles were conducted in duplicate, while LMW peptide profiles and SCFAs analysis were performed in triplicate for each batch of samples. Statistical analyses were carried out using R version 4.2.2 (R Development Core Team). One-way ANOVA with individual post hoc comparisons with the Tukey–Kramer test was applied to SCFAs and LMW peptide data, highlighting statistically significant differences among different sampling points within each SHIME® line. Student's *t*-test was used for comparing AAs profiles, IVPD, and PDCAAS data means between RRLPI and FRLPI, and to compare SCFAs and LMW peptides data between PC1 and PC2, and between DC1 and DC2 at various sampling times. A significant level of 5 % was used for all hypothesis tests.

The Shannon Diversity Index (SDI) was calculated from microbial count data, and group-wise differences in alpha diversity (SDI) were assessed using Kruskal–Wallis test followed by pairwise Wilcoxon test, with *p*-values adjusted for multiple comparisons via the Benjamini–Hochberg procedure. Beta diversity was assessed using Bray–Curtis dissimilarities based on genus-level relative abundances (filtered to include taxa with >0.001 % abundance) and visualized through principal coordinate analysis (PCoA). Differences in community structure across groups were evaluated using permutational multivariate analysis of variance (PERMANOVA) with the *adonis2* function. Differentially abundant taxa between treatments and sampling time points (T1, T2, T3 vs. T0) were identified using Maaslin2 (Mallick et al., 2021).

Identified LMW peptides were subjected to differential abundance analysis in MetaboAnalyst 6.0 (Pang et al., 2024). Peptides significantly altered during the treatment period of SHIME experiment (T1+T2) between the lines fed with FRLPI and RRLPI were identified through fold-change analysis combined with *t*-tests, adjusted for false discovery rate (FDR), and visualized in volcano plots.

To investigate treatment and temporal patterns and to identify variables contributing to group differentiation, multivariate analyses were performed. These included Partial Least Squares Discriminant Analysis (PLS-DA) and Principal Component Analysis (PCA) biplots, utilizing data from the 20 most abundant genera, SCFAs, and significantly different BPs. All data were normalized and scaled prior to analysis, and visualizations were generated using the mixOmics and factextra packages in R.

3. Results

3.1. RLPI digestibility

Fermentation of RLPI significantly ($p < 0.05$) altered the amino acid profile, as shown in Table 1. Among essential amino acids (EAAs), L-Threonine (Thr) was significantly higher in FRLPI compared to RRLPI (2.93 ± 0.07 vs. 2.38 ± 0.04). In contrast, L-Cysteine (Cys) + L-Methionine (Met), L-Leucine (Leu), and L-Lysine (Lys) were significantly higher in RRLPI than in FRLPI (3.83 ± 0.07 , 5.52 ± 0.06 , and 4.70 ± 0.14 , respectively).

For non-essential amino acids (NEAAs), the impact of fermentation was more variable. Although several NEAAs increased numerically in FRLPI, only L-Glutamic Acid (Glu) and L-Proline (Pro) were significantly higher compared to RRLPI (16.05 ± 0.24 vs. 13.18 ± 1.45 and 3.18 ± 0.04 vs. 2.80 ± 0.20 , respectively). Conversely, L-Serine (Ser), L-Glycine (Gly), L-Alanine (Ala), and L-Arginine (Arg) were significantly more abundant in RRLPI (4.17 ± 0.05 , 2.88 ± 0.11 , 2.88 ± 0.16 , and 6.30 ± 0.04 , respectively). The positive effect of the fermentation was more evident when results were expressed per gram of protein

(Supplementary Table 1). Thr, L-Valine (Val), Leu, Lys, L-Histidine (His), L-Aspartic Acid (Asp), Glu, Pro, Ala, and Arg were higher in FRLPI compared to RRLPI. L-Tryptophan (Trp) increased slightly, while Gly and Cys + Met decreased.

Fermentation also significantly improved the IVPD, increasing from 92.5 ± 0.7 % in RRLPI to 94.5 ± 0.7 % in FRLPI ($p < 0.05$). Although Trp remained the first limiting amino acid in both samples, the AAS and PDCAAS values were slightly higher in FRLPI (0.41 ± 0.02 and 0.39 ± 0.02) compared to RRLPI (0.39 ± 0.04 and 0.37 ± 0.03), though these differences were not statistically significant.

3.2. Modulation of SCFAs production

At the end of the control period (T0), no significant differences were found in SCFAs concentrations between the two SHIME® lines in either colon tract (Table 2). However, the administration of both FRLPI and RRLPI significantly increased SCFAs concentrations ($p < 0.05$) during the treatment phase (T1 and T2), followed by a significant decrease after the washout period (T3). Acetic acid concentrations significantly increased ($p < 0.05$) at T1 and T2 compared to T0 in both PC and DC bioreactors. Following washout (T3), levels decreased significantly ($p < 0.05$) but remained higher than T0 in the PC bioreactor fed with FRLPI ($p < 0.05$). In the DC bioreactors, both FRLPI and RRLPI treatments

Table 2

Short chain fatty acids (SCFAs) concentrations (mM) in proximal colon (PC) and distal colon (DC) bioreactors at baseline (T0), during one and two weeks of treatment period (T1, T2), and after washout (T3). SHIME® lines were fed with fermented (FRLPI) or raw (RRLPI) red lentil protein isolate. Statistical analysis was performed using one-way ANOVA with Tukey-Kramer post hoc tests for temporal changes within each bioreactor, and Student's *t*-test for comparisons between two SHIME® lines at each time point. In the same column, values with different superscript letters indicate significant temporal differences ($p < 0.05$). For each bioreactor, values in the same line with asterisk indicate significant differences between different feeding regimen ($p < 0.05$). Values are means \pm standard deviation ($n = 3$).

Acetic acid (mM)				
	PC		DC	
	FRLPI	RRLPI	FRLPI	RRLPI
T0	25.62 \pm 1.35 _c	23.52 \pm 2.16 _b	T0 41.62 \pm 0.73 ^d	45.84 \pm 0.80 ^c
T1	47.14 \pm 2.13 _a	44.60 \pm 2.22 _a	T1 82.16 \pm 1.17 ^b	86.62 \pm 1.53 ^{b/*}
T2	50.52 \pm 1.89 _a	48.46 \pm 1.91 _a	T2 97.82 \pm 3.49 ^a	107.30 \pm 4.40 ^{a/*}
T3	31.19 \pm 1.59 _b	26.79 \pm 2.27 _b	T3 60.97 \pm 7.90 ^{c/*}	47.08 \pm 0.33 ^c
Propionic acid (mM)				
	PC		DC	
	FRLPI	RRLPI	FRLPI	RRLPI
T0	13.01 \pm 0.47 ^b	14.93 \pm 1.10 ^b	T0 20.10 \pm 0.45 ^b	21.62 \pm 1.32 ^b
T1	29.45 \pm 1.85 ^a	29.54 \pm 0.96 ^a	T1 41.35 \pm 0.50 ^a	41.98 \pm 1.59 ^a
T2	32.13 \pm 0.83 ^a	30.26 \pm 2.02 ^a	T2 39.92 \pm 0.47 ^a	42.89 \pm 0.94 ^{a/*}
T3	7.75 \pm 0.32 ^c	7.99 \pm 0.40 ^c	T3 13.82 \pm 1.09 ^c	12.48 \pm 0.46 ^c
Butyric acid (mM)				
	PC		DC	
	FRLPI	RRLPI	FRLPI	RRLPI
T0	13.86 \pm 0.31 _b	13.80 \pm 0.66 ^c	T0 16.73 \pm 0.60 ^c	15.89 \pm 0.87 ^c
T1	83.24 \pm 0.21 _{a/*}	73.55 \pm 0.99 ^a	T1 107.85 \pm 1.43 _{a/*}	100.97 \pm 2.35 _a
T2	84.85 \pm 1.03 _{a/*}	76.57 \pm 2.87 ^a	T2 107.14 \pm 1.14 _{a/*}	100.60 \pm 0.75 _a
T3	14.51 \pm 0.58 _b	19.58 \pm 0.90 _{b/*}	T3 21.30 \pm 1.12 ^b	25.28 \pm 0.76 _{b/*}

Table 1

Amino acid (AA) concentrations (g/100 g of sample), in vitro protein digestibility (IVPD %), first limiting amino acid, amino acid score, and protein digestibility-corrected amino acid score (PDCAAS) in fermented (FRLPI) and raw (RRLPI) red lentil protein isolates. Values represent means \pm standard deviation ($n = 2$) of two biological replicates. Statistical analysis was performed using Student's *t*-test. Values in the same row with an asterisk (*) indicate significant differences between groups ($p < 0.05$).

AMINO ACIDS (g/100 g of sample)	FRLPI	RRLPI
Essential Amino acids (EAAs)		
L-Cysteine (Cys) + L-Methionine (Met)	1.73 \pm 0.12	3.83 \pm 0.07 *
L-Tryptophan (Trp)	0.23 \pm 0.02	0.36 \pm 0.04
L-Threonine (Thr)	2.93 \pm 0.07	2.38 \pm 0.04*
L-Valine (Val)	2.76 \pm 0.16	2.45 \pm 0.14
L-Isoleucine (Ile)	2.1 \pm 0.13	2.20 \pm 0.14
L-Leucine (Leu)	4.71 \pm 0.07	5.52 \pm 0.06 *
L-Tyrosine (Tyr) + L-Phenylalanine (Phe)	4.06 \pm 0.07	5.82 \pm 0.93
L-Lysine (Lys)	3.15 \pm 0.2	4.70 \pm 0.14 *
L-Histidine (His)	1.54 \pm 0.14	1.82 \pm 0.06
Nonessential Amino Acids (NEAAs)		
L-Aspartic acid (Asp)	9.11 \pm 0.33	7.72 \pm 1.25
L-Serine (Ser)	3.33 \pm 0.15	4.17 \pm 0.05*
L-Glutamic Acid (Glu)	16.05 \pm 0.24	13.18 \pm 1.45*
L-Proline (Pro)	3.18 \pm 0.04	2.80 \pm 0.20*
L-Glycine (Gly)	1.66 \pm 0.11	2.88 \pm 0.11*
L-Alanine (Ala)	1.93 \pm 0.07	2.88 \pm 0.16*
L-Arginine (Arg)	5.11 \pm 0.33	6.30 \pm 0.04*
IVPD %	94.5 \pm 0.7	92.5 \pm 0.7*
First limiting amino acid	L-Tryptophan	L-Tryptophan
Amino acid score	0.41 \pm 0.02	0.39 \pm 0.04
PDCAAS	0.39 \pm 0.02	0.37 \pm 0.03

demonstrated a significant increase in acetate concentrations from T1 to T2. Notably, the RRLPI treatment consistently resulted in higher acetate levels at both time points compared to the FRLPI treatment ($p < 0.05$). At T3, acetate levels in the DC bioreactor fed with FRLPI remained higher than those observed in the RRLPI-fed bioreactor. Propionic acid followed a similar trend, with concentrations significantly increasing ($p < 0.05$) at T1 compared to T0 in all colon tracts. However, no significant differences were observed between T1 and T2 for either treatment. At T2, propionic acid levels in the DC bioreactor were significantly higher ($p < 0.05$) after feeding with RRLPI compared to FRLPI. After the washout (T3), propionic acid levels were significantly lower ($p < 0.05$) than the treatment period in all bioreactors. Butyric acid concentrations significantly increased ($p < 0.05$) at T1 compared to T0 across all

bioreactors. However, FRLPI-fed bioreactors showed significantly higher levels at T1 and T2 compared to the RRLPI-fed bioreactors ($p < 0.05$). In contrast, at T3, butyric acid levels decreased significantly, but not compared to baseline, and were lower ($p < 0.05$) in bioreactors fed with FRLPI than in those fed with RRLPI. Exception was for the PC bioreactor fed with FRLPI.

3.3. Temporal dynamics of peptides and bioactive peptides in the gut ecosystem

The total abundance of LMWP (4–30 AAs), expressed as ion intensity (A.U.), was monitored over time in the PC and DC bioreactors to evaluate peptide evolution in response to feeding with FRLPI and RRLPI

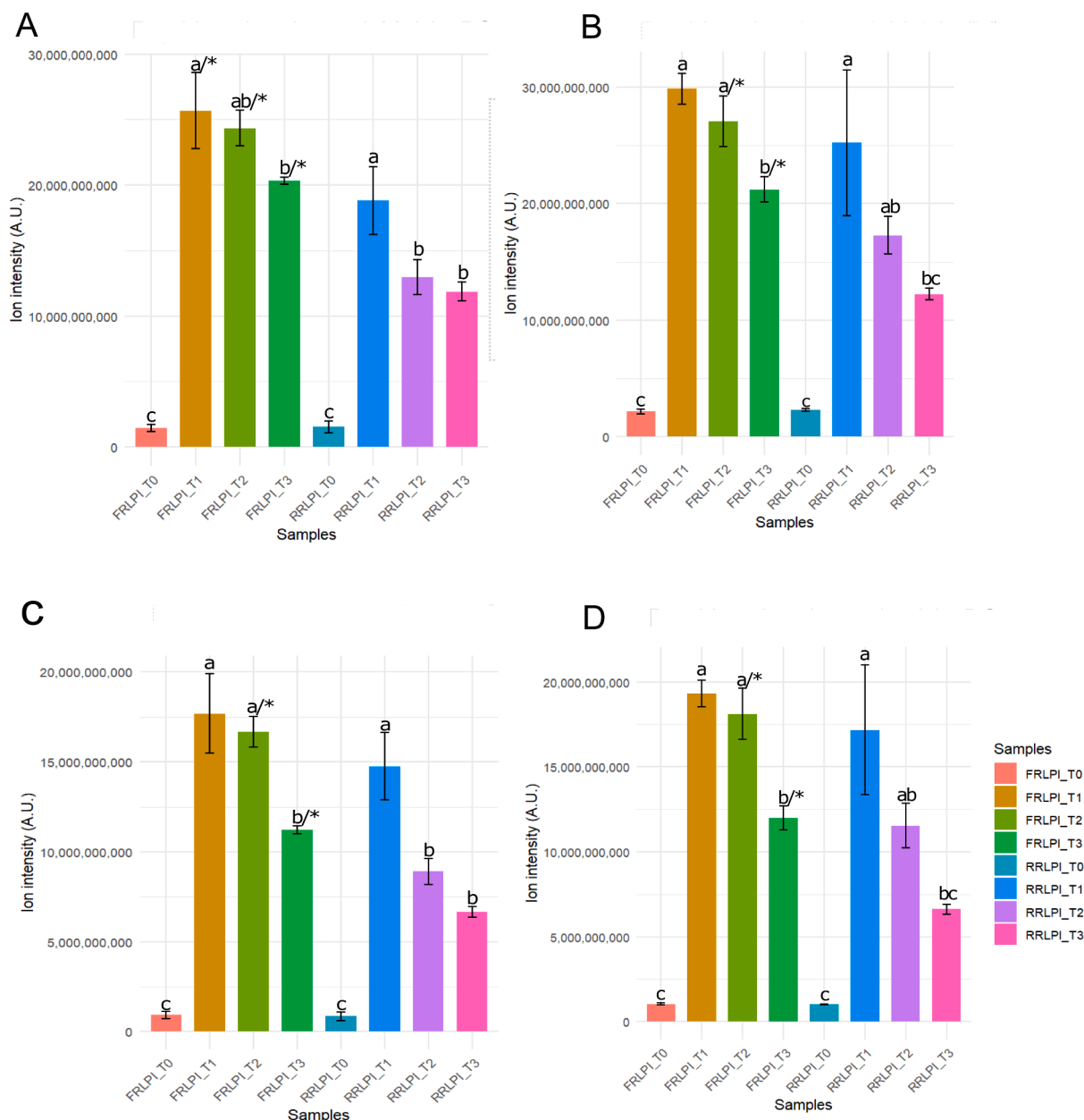


Fig. 1. Temporal and treatment-dependent variations in low molecular weight peptides (LMWP) in the SHIME® model. Panels A and B show the total abundance (ion intensity, A.U.) of LMWP ranging from 4 to 30 amino acids in the proximal colon (PC) and distal colon (DC) bioreactors, respectively. Panels C and D detail the abundance of shorter LMWP (4–7 amino acids) in the PC and DC. Measurements were taken at baseline (T0), after one week (T1), two weeks (T2) of feeding with either fermented (FRLPI) or raw (RRLPI) red lentil protein isolate, and after one week of washout (T3). For each graph, bars with different letters differ significantly according to one-way ANOVA with Tukey-Kramer post hoc tests for multiple comparisons ($p < 0.05$). Differences between treatments (FRLPI vs. RRLPI) at each time point were assessed using Student's *t*-test ($p < 0.05$; * indicates significance).

(Fig. 1A and 1B). At baseline (T0), no significant differences in total peptide abundance were found between the SHIME® lines in either bioreactor. During the treatment phase, the intake of both FRLPI and RRLPI caused a significant ($p < 0.05$) increase in total peptide abundance compared to baseline (T0). These elevated levels persisted after the washout period (T3), except in the DC bioreactor fed with RRLPI. When comparing the different treatments at each time point, FRLPI administration in the PC bioreactor resulted in a significantly higher ($p < 0.05$) total peptide abundance than RRLPI at T1, T2, and after the washout period (T3). In contrast, within the DC bioreactor, FRLPI intake significantly increased peptide abundance compared to RRLPI only at T2 and T3.

BPs, ranging from 4 to 7 amino acids (AAs), were detected, and validated at all time points in both PC and DC bioreactors. A total of 11 BP sequences were identified (Supplementary Table 2). To ensure robust analysis, the fecal sample from the donor was also examined, where a single peptide sequence (QPGR) was detected. At T0, this sequence was found in both the PC and DC bioreactors of both SHIME® lines.

In the SHIME® line fed with FRLPI, in the PC bioreactor 11 BP sequences were found at T1, decreasing to 8 at T2. Concurrently, in the DC bioreactor, the counts were 7 at T1 and remained steady at 8 BP sequences at T2. After a one-week washout period (T3), the number of BPs

sequences dropped to 5 and 2 in the PC and DC, respectively. For the SHIME® line fed with RRLPI, 9 and 8 BP sequences were identified in the PC bioreactor at T1 and T2, respectively, while 8 and 9 sequences were observed in the DC bioreactor at the same time points. After the washout period (T3), the BP sequences decreased to 5 and 3 in PC and DC, respectively.

In the SHIME® line fed with FRLPI, the total abundance of BPs (4–7 AAs) in both PC and DC significantly increased in the treatment period (T1 and T2) compared to baseline (T0) (Fig. 1C and D). At T3, the levels decreased, but they were still significantly higher than T0. For the RRLPI-fed SHIME® line, the total peptide abundance also increased significantly at T1 and T2 compared to T0 in both PC and DC, and the levels remained significantly higher also at T3. Overall, FRLPI feeding led to a more sustained increase in BP abundance, particularly in the PC, even after the washout period.

Differential peptide abundance between the SHIME lines fed with FRLPI and RRLPI during the treatment period (T1 and T2) was identified through statistical analysis and visualized using volcano plots (Fig. 2A and B). In the PC (Fig. 2A), a total of 8541 peptides showed significant changes in abundance respective to FRLPI feeding. Peptides with the highest increased abundance included PAGHP, KIGRH, and HCKNKA, with \log_2 fold changes ranging from 6.8 to 7.5. Similarly, BPs such as

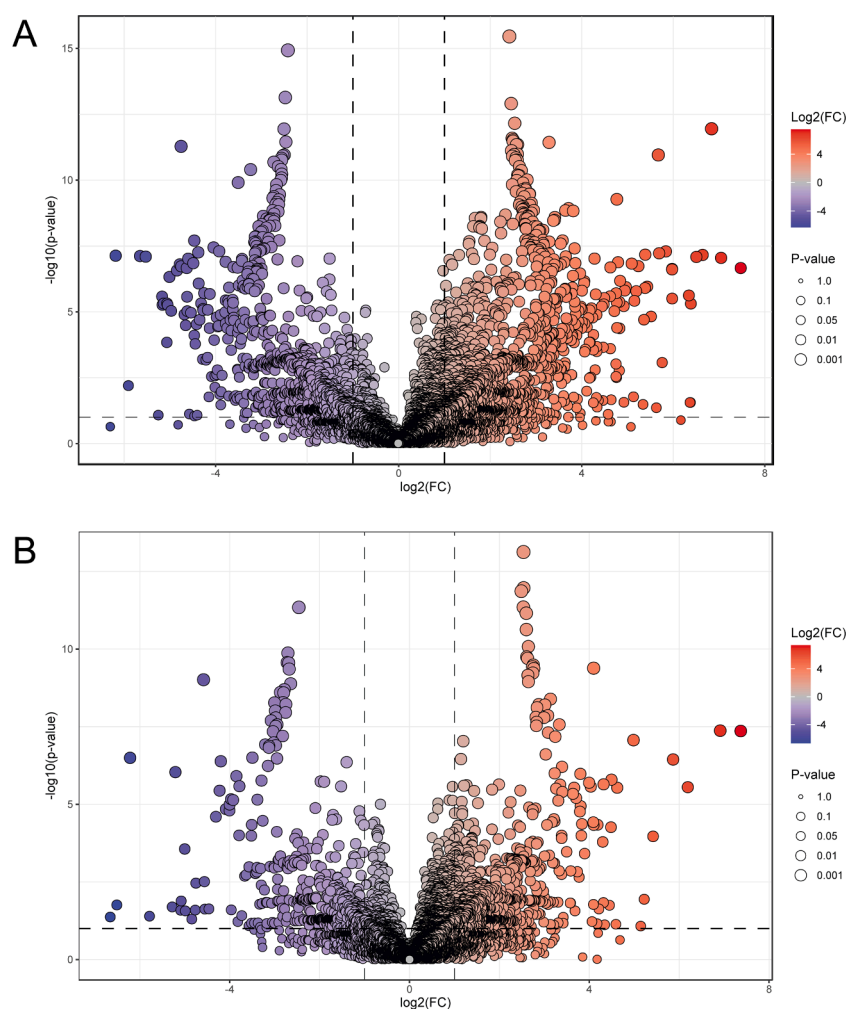


Fig. 2. Volcano plots illustrating significant ($p < 0.05$) differences in peptide abundances between two feeding regimen in the SHIME® model. Peptide abundances in the proximal colon (Panel A) and distal colon (Panel B) after one week (T1) and two weeks (T2) of treatment. The SHIME® lines were fed with fermented red lentil protein isolate (FRLPI) and raw red lentil protein isolate (RRLPI). Each point on the plot represents an individual peptide. The x-axis shows the \log_2 fold change, indicating relative abundance differences between treatments (FRLPI vs. RRLPI), while the y-axis shows the $-\log_{10}$ (p-value), representing the statistical significance of these differences. Peptides above the significance threshold are color-coded to indicate a positive or negative fold change in the FRLPI-fed samples compared to the RRLPI-fed samples.

QPGR, HIRL, TERGY, PPPP, and AGDDAPR showed increased abundance, with \log_2 fold changes between 1.1 and 2.3 in FRLPI-fed samples. Conversely, a subset of peptides showed decreased abundance in FRLPI-fed samples, including HPSV and KQEEKVER, with \log_2 fold changes of approximately -2.4 . In the DC (Fig. 2B), 4476 peptides showed significant changes in abundance compared to FRLPI feeding. Among these, peptides such as FSTLT, PMHLR, EPVVQP, and EVNLPP increased notably, with \log_2 fold changes of about 2.5. The peptides TPRNR, TPEALI, and VVEISP showed the largest overall increases, with \log_2 fold changes reaching 7.4. In contrast, certain peptides demonstrated decreased abundance in FRLPI-fed samples compared to RRLPI, including VFSKL, EPIDLS, and LDSLPE, with \log_2 fold changes of approximately -6.7 . Additionally, BPs such as QPGR and VIEPR exhibited increased abundance, with \log_2 fold changes ranging between 1.1 and 3.

3.4. Interplay between RLPI treatments and microbial composition, diversity, and functionality

Fig. 3A shows the 20 most abundant bacterial genera in the PC and DC for each SHIME® line. At baseline (T0), the PC was dominated by *Bifidobacterium* (38–56 %), followed by *Collinsella* (9–11 %), *Dialister* (7–9 %), *Enterococcus* (7–9 %), and *Bilophila* (5–9 %). In contrast, the DC had higher relative abundances of *Blautia* (17–29 %), *Bifidobacterium*

(6–20 %), *Bacteroides* (10–12 %), *Ruminococcus* (5–13 %), and *Collinsella* (6 %). During the treatment period (T1 and T2), *Lactiplantibacillus* consistently increased in both PC and DC, with a stronger effect observed after feeding with FRLPI, particularly in the DC, while the feeding with RRLPI led to a delayed increase at T2. *Blautia* showed a steady rise in the PC, but its abundance decreased in the DC during the same period. *Furfurilactobacillus* showed a transient increase, peaking at T1 in the PC and at T1 or T2 in the DC, depending on the treatment, before disappearing by T3. *Lactobacillus* increased in the PC fed with FRLPI at T1, whereas the intake of RRLPI resulted in a later increase in DC (observed at T2 and T3). Conversely, *Bifidobacterium* generally decreased during the treatment period in both PC and DC, though it began recovering at T3, particularly in the DC fed with RRLPI. A treatment-specific and colon tract-dependent microbial shift during and after FRLPI and RRLPI administration was found.

The Shannon diversity index revealed no significant changes in alpha diversity over time for either treatment or colon tract. The PCoA plots (Fig. 3B) showed clear temporal shifts in beta diversity. In the PC, microbial composition evolved over time, with T0 clustering separately, T1 and T2 grouping closely, and T3 forming a distinct cluster after washout. In DC, the evolution of bacterial communities was more impacted by the feeding regimen. The feeding with FRLPI showed distinct clustering at T1 and T2, while the microbial composition shifted back to baseline (T0) after washout (T3). The intake of RRLPI resulted in a pronounced

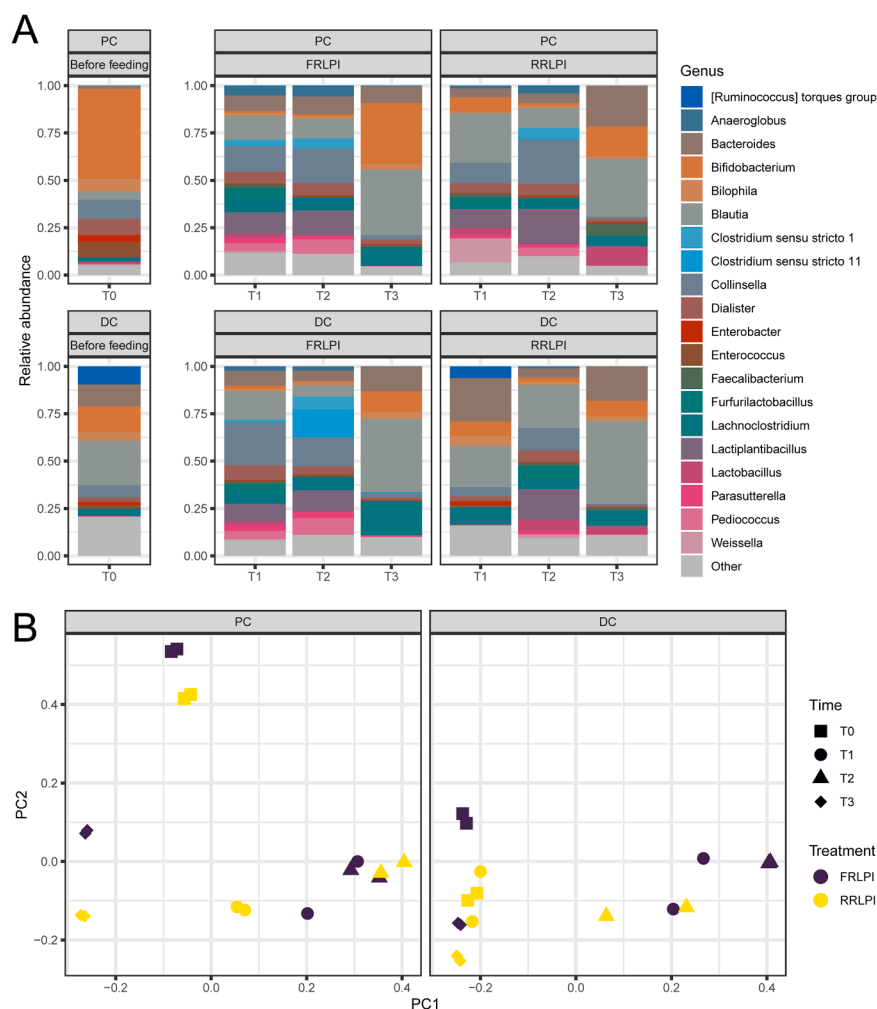


Fig. 3. Dynamics of bacterial genera abundances and microbial community structures in SHIME® bioreactors. Panel A illustrates the 20 most abundant bacterial genera in the proximal colon (PC) and distal colon (DC) at baseline (T0), and after seven days (T1), fourteen days (T2) of treatment with fermented (FRLPI) and raw (RRLPI) red lentil protein isolates, followed by one week of washout (T3). Panel B presents Principal Coordinate Analysis (PCoA) plots that visualize the dynamics of microbial community structures based on relative abundances of these genera in the PC and DC across the same time points and treatments.

clustering at T2, whereas T0, T1, and T3 displayed greater overlap, indicating less sustained temporal changes.

The MaAsLin analysis comparing microbial composition between FRLPI and RRLPI treatments, independent of time, revealed no significant differences. However, temporal analysis showed notable changes during the treatment phases (T1 and T2) as well as the washout phase (T3). In the PC, significant changes were observed over time. During the treatment period, *Lactiplantibacillus* and *Furfurilactobacillus* showed increased relative abundance in response to FRLPI intake, while *Blautia* and *Collinsella* were enriched in response to RRLPI. After the washout phase (T3), *Blautia* and *Collinsella* remained elevated with both treatments, indicating recovery or stabilization. In contrast, *Lactiplantibacillus* and *Furfurilactobacillus* exhibited a marked decline, reflecting the transient nature of their enrichment during intervention. In DC, no significant differences were detected during the treatment period, while the most prominent microbial changes occurred during the washout phase. In fact, at T3, significant differences emerged ($q < 0.05$), with *Lactiplantibacillus* and *Blautia* showing increased relative abundance in response to the feeding with FRLPI, while *Bifidobacterium* exhibited a recovery trend across both treatments. Cumulatively these results indicate that microbial responses in the PC were dynamic throughout the treatment period, while changes in the DC were delayed and became noticeable mainly after the treatment ended.

The supervised PLS-DA (sPLS-DA) plots (Fig. 4A and B) revealed clear temporal and treatment-driven separations in both the PC and DC. At T2, FRLPI and RRLPI-treated samples diverged significantly in both colon tracts, highlighting distinct effects of the two-feeding regimen on

microbial and metabolite profiles. At T3 (washout), although both treatments shifted closer to baseline, the separation persisted, with FRLPI samples forming tighter clusters compared to the more dispersed RRLPI samples. These findings suggest that FRLPI induced more distinct and transient changes, while RRLPI effects were more gradual and variable. The PCA biplots (Fig. 4C and D) complemented these findings by visualizing associations between bacterial genera, SCFAs, and significant BPs with specific treatments and time points. In the PC (Fig. 4C), baseline samples (T0) cluster separately from treatment samples, reflecting minimal association with increased SCFAs or peptides. During the treatment period (T1, T2), FRLPI samples align with elevated SCFAs levels (e.g., acetic acid, propionic acid) and BPs such as AGDDAPR. This shift was also associated with an increased relative abundance of *Lactiplantibacillus* and *Furfurilactobacillus*. Conversely, RRLPI samples were linked to *Weissella* and *Parasutterella* genera, along with BPs like PPPP and TERGY. By T3, samples from both treatments shift toward baseline conditions, with FRLPI-treated samples showing a more pronounced return, indicated by clustering closer to *Bifidobacterium* and *Lactobacillus*. In the DC (Fig. 4D), a similar trend was observed, with baseline samples (T0) distinctly separated from those of the treatment and washout phases. During T1 and T2, FRLPI treatment was associated with elevated SCFAs, BPs (e.g., VIEPR), and microbial *Lactiplantibacillus*, *Pediococcus*, and *Anaeroglobus* taxa. At T2, RRLPI samples clustered separately from others and were associated with the genera *Collinsella*, *Furfurilactobacillus*, and *Bacteroides*. By T3, both treatment groups exhibited a movement toward baseline conditions. Samples treated with FRLPI clustered closely with *Bifidobacterium* and *Blautia*, reflecting a

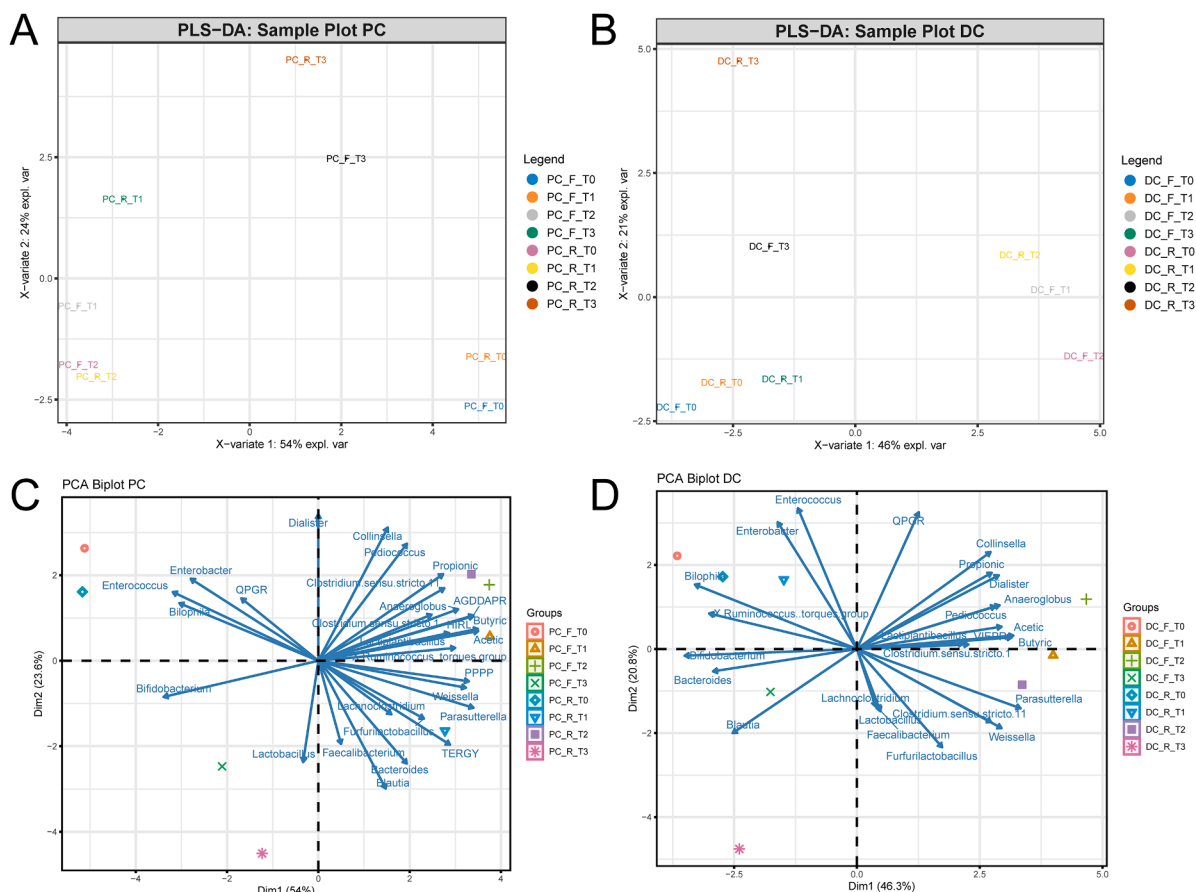


Fig. 4. Multivariate analyses of microbial and metabolic profiles in proximal (PC) and distal colon (DC) compartments. Panels A and B show Partial Least Squares Discriminant Analysis (PLS-DA) plots illustrating temporal and treatment-related distinctions within PC and DC, respectively, across different treatment periods with fermented red lentil protein isolate (FRLPI) and raw red lentil protein isolate (RRLPI). Panels C and D present Principal Component Analysis (PCA) biplots that highlight associations between the 20 most abundant bacterial genera, short-chain fatty acids (SCFAs), and significantly different bioactive peptides (BPs) for PC and DC, respectively, indicating the interactions across treatment and time points.

more rapid microbiota recovery to baseline. In contrast, RRLPI-treated samples remained more widely dispersed, indicating a gradual return to baseline of both microbial communities and metabolite profiles.

4. Discussion

The selection of RLPI fermented by *H. uvarum* SY1 was based on our prior findings (Tonini et al., 2024), which highlighted the proteolytic capability of *H. uvarum* SY1 and promoted release of BPs during fermentation. The released BPs in the prior study have shown significant ACE inhibitory and antioxidant activities, which contribute to managing hypertension and quenching oxidative stress. Our study brings further insights beyond these aspects by investigating the protein digestibility and the impact of both fermented and raw RLPI on the human gut microbiota, including the modulation of BPs release during digestion.

Fermentation significantly altered the AA profile of RLPI (Table 1). Among EAAs, Thr was notably higher in FRLPI, whereas Cys, Met, Leu, and Lys were more abundant in RRLPI. These shifts reflect the proteolytic activity of *H. uvarum* SY1, known to preferentially utilize sulfur-containing amino acids such as Met and Cys as nitrogen sources (Tonini et al., 2024; Ciani et al., 2019; Comitini et al., 2021; Onetto et al., 2025).

Regarding non-essential amino acids (NEAAs), Glu and Pro increased in FRLPI, while Ser, Gly, Ala, and Arg decreased. These alterations align with *H. uvarum*'s selective uptake and metabolic conversion of specific AAs, notably through pathways such as Ehrlich fermentation, leading to their reduction (Lleixà et al., 2019; Badura et al., 2023; Kemsawasd et al., 2015). The accumulation of Glu and Pro likely results from the yeast's biosynthetic activities and distinct nitrogen metabolism. Expressed per gram of protein, FRLPI exhibited substantially higher levels of key EAAs, including Thr, Val, Ile, Leu, Lys, His, and Phe + Tyr, surpassing the FAO/WHO adult dietary requirements (Paoletti et al., 2024). Although levels of Met + Cys and Trp were lower, the overall improved EAA profile in FRLPI indicates enhanced nutritional quality driven by fermentation-induced proteolysis and microbial synthesis (Sun et al., 2025). Additionally, increases in NEAAs like Glu, Asp, and Pro further suggest a functional enhancement of the protein matrix.

Fermentation significantly improved the IVPD of RLPI from $92.5 \pm 0.7\%$ to $94.5 \pm 0.7\%$ ($p < 0.05$), reflecting enhanced protein hydrolysis. Although Trp remained the limiting amino acid, AAS and PDCAAS were slightly higher in FRLPI than in RRLPI, though not significantly. Reported PDCAAS values for red lentils typically range between 0.54–0.59 for cooked whole seeds and flours (Nosworthy et al., 2023, 2017), and can reach 0.63–0.64 when extruded. These higher values are often associated with thermal processing, which improves protein digestibility and amino acid availability. In contrast, the PDCAAS values observed in our study for RRLPI (0.37) and FRLPI (0.39) were lower. This discrepancy can be attributed to several factors. First, we used protein isolates, which may differ in amino acid composition and matrix effects compared to whole lentils or flours (Nosworthy et al., 2023). Second, our samples did not undergo heat processing, which has been shown to enhance digestibility in lentil proteins (Hall and Moraru, 2021). Third, fermentation can modulate amino acid availability by microbial consumption or transformation, as observed with reduced levels of Lys and Cys in FRLPI (Diether and Willing, 2019). Finally, differences in PDCAAS values may also arise from methodological variables, such as the use of *in vitro* digestion models and reference scoring patterns (Sá et al., 2023). These factors collectively explain the lower PDCAAS and AAS values in our isolates, while still providing a relevant comparison for evaluating functional shifts due to fermentation.

The impacts of feeding with FRLPI and RRLPI on gut microbiota composition and metabolic responses were studied using the SHIME® model, a reliable dynamic *in vitro* gut ecosystem simulator that eliminates interference from other dietary habits and host-dependent physiological factors (Polo et al., 2023). Both lentil protein isolates were administered at a daily dose of 37.8 g of substrate, reflecting protein

intakes of approximately 31.37 g (RRLPI) and 19.28 g (FRLPI). This dosage was chosen to accommodate the low solubility of RLPI for the requirements of the *in vitro* system and to align with current trends towards sustainable, plant-based protein sources (Kuesten, 2020), rather than to meet full daily protein requirements. Further, proteins were pre-digested prior to administration into the colon vessels of the SHIME® system, and no absorption compartment was included. While this deviates from *in vivo* physiology, where most dietary proteins are absorbed in the small intestine, pre-digestion was necessary to avoid the cytotoxic effects associated with high loads of intact protein in the colon, which have been previously reported to negatively impact microbial viability and metabolic activity (Diether and Willing, 2019; Gilbert et al., 2018). Moreover, the low molecular weight peptide fraction (<3 kDa) obtained after digestion resembles the pool of bioavailable peptides likely to escape small intestinal absorption and reach the colon (Keller, 2013). Thus, although the lack of a simulated absorption step represents a limitation, the chosen approach ensured microbial safety and provided a physiologically relevant peptide profile for evaluating colonic microbial responses.

The uniform SCFAs levels at the baseline confirmed the stability and reproducibility of gut environment between two SHIME® lines, allowing for a controlled assessment of impacts by feeding with fermented and raw RLPI (Van de Wiele et al., 2015). The observed increase in SCFA production likely reflects the higher fermentable protein input from LPI supplementation (31.37 g/day for RRLPI, 19.28 g/day for FRLPI), which markedly exceeded the basal feed's protein content (2.06 g/day). Although SCFAs synthesis was mainly associated with carbohydrate fermentation, our findings highlighted the significant contribution of amino acids metabolism. In fact, several amino acids, such as Gly, Thr, and Lys, provide alternative substrates for SCFAs production when carbohydrate availability is low (Martin-Gallausiaux et al., 2021). The enhanced SCFAs production in DC compared to the PC underscored the influence of local pH and microbial density on fermentation. This tract-specific activity supports the notion that a near-neutral pH favors proteolytic fermentation, which is crucial for SCFAs production (Neis et al., 2015).

The notable increase in butyric acid concentration following FRLPI treatment may be influenced by microbial fermentation of amino acids known to contribute to butyrate production, including Thr, Lys, Glu, and Val (Neis et al., 2015). Although not all of these amino acids were elevated in FRLPI, their presence, alongside the fermentative metabolism initiated during protein fermentation, may have supported enhanced butyrogenesis in the colon compartment. Butyrate plays a significant role in gut health since it is known for its anti-inflammatory properties and ability to strengthen gut barrier function. These benefits are instrumental in preventing diseases such as colorectal cancer and irritable bowel syndrome, highlighting the broader implications of optimized amino acid intake for maintaining intestinal health (Louis et al., 2017; Fung et al., 2012; Blaak et al., 2020).

Building on the demonstrated health-promoting potential of BPs in FRLPI (Tonini et al., 2024), here we investigated their release during the simulation of colonic fermentation. A consistent increase in LMWPs was observed in colon tracts during both treatment (i.e., intake of FRLPI and RRLPI) and washout phases, especially in samples from the SHIME® line fed with FRLPI. This enhancement can be attributable to the proteolytic activity of *H. uvarum* (Ciani and Comitini, 2019). Besides, fermentation has been shown to improve the solubility of pulse proteins (Liu et al., 2023), enhancing their availability for enzymatic hydrolysis and microbial metabolism in the gut. In contrast, insoluble proteins are more resistant to degradation by the colonic microbiota (Macfarlane and Allison, 1986).

The identified BPs in lumen samples differed from those detected in the original FRLPI substrate (Tonini et al., 2024), likely due to further structural modifications by colonic fermentation. This transformation potentially underscores the dynamic interaction between dietary peptides and gut microbiota, which can lead to varied bioactivities within

the gut environment (Amigo et al., 2020). Despite the speculative nature of the bioactivities based on sequence analysis and literature, the identified peptides, such as AGDDAPR and QAFT, are linked to ACE inhibitory and antioxidant functions. These functions suggest potential benefits in managing hypertension and reducing oxidative stress, respectively (Wu et al., 2017; Zhu et al., 2022). Additionally, peptides like QPGR demonstrate potential α -glucosidase inhibitory activity, which may assist in managing glucose levels post-meals (Hedrington et al., 2019).

Concerning the gut microbial ecosystem, the balance between potentially beneficial and detrimental effects on host health is intricately linked to the diversity, abundance, and distribution of microbiota taxa (Liu et al., 2021). We highlighted colon tract-specific responses of gut microbiota to dietary interventions by the PCoA plots, emphasizing the dynamic nature of these communities in response to changes in available nutrients (Yao et al., 2023). Prior to treatment, the bacterial community was dominated by genera commonly identified within the human gut (Rinninella et al., 2019). In the PC, transient shifts observed during treatment phases, particularly after feeding with FRLPI, stabilized during the washout, indicating a robust but reversible microbial response to substrate administration (Fassarella et al., 2021). These shifts underscore the microbiota adaptability and its potential to return to a pre-treatment state, a resilience further evidenced by recovery patterns noted in dietary intervention studies (Walker et al., 2011; Lozupone et al., 2012). Conversely, the DC exhibited delayed and less pronounced changes, particularly in response to feeding with RRLPI, suggesting that short-term interventions might be insufficient to induce significant and lasting shifts in this colon tract (Minnebo et al., 2023).

The evolution of bacteria communities during the simulation revealed notable shifts in genera abundance between treatments, identifying significant changes particularly associated with FRLPI administration. *Lactiplantibacillus* and *Furfurilactobacillus* which were linked to the enhanced release of SCFAs and BPs (AGDDAPR and VIEPR), and *Bacteroides* increased after FRLPI intake. These findings highlight the proteolytic capabilities of the identified genera, which facilitate the bioavailability of BPs, and thereby may contribute to immune modulation and pathogen inhibition (Garcia-Gonzalez et al., 2021). *Lactiplantibacillus*, that proliferated in response to longer-term FRLPI intake, is widely recognized for its probiotic effects in the human gastrointestinal tract, as evidenced by clinical studies (Qin et al., 2022). The potential health benefits conferred by this genus are manifold; they include modulation of the commensal microbiota, inhibition of pathogenic bacteria, enhancement of intestinal barrier function via mucin production, immune system modulation, and the production of health-promoting bioactive molecules (Garcia-Gonzalez et al., 2021). Although the analysis did not achieve species-level identification, also *Furfurilactobacillus* genus belongs to the Lactobacillaceae family, renowned for its health-promoting properties like production of secondary metabolites, the synthesis of bioactive compounds, and other complex biochemical pathways, each playing a pivotal role in health betterment (Walter et al., 2023; Palomino et al., 2023). *Bacteroides* has been linked to proteolytic activity in the large intestine and increased relative abundance under high-protein diets (Moreno-Pérez et al. 2018), while as a gut commensal is a genus renowned for helping guard against pathogens and support other microbial inhabitants of the gut (Zafar et al., 2021).

Conversely, the intake of RRLPI resulted in an increased level of *Blautia* and *Collinsella* genera, while the PCA biplots associated this feeding to further taxa such as *Weissella*, *Parasutterella* and the release of BPs (PPP and TERGY). BPs associated with the bacterial taxa have potential antioxidant and ACE inhibitory activity (Grancieri et al., 2019; Ngo et al., 2023). *Blautia* is a prevalent genus within the gut microbiota postulated for its potential probiotic functions, including the production of bacteriocins with antimicrobial properties (Liu et al., 2021). This genus has also been shown to negatively correlate with visceral fat accumulation, suggesting its potential role in metabolic health (Ozato

et al., 2019). However, an elevated abundance of *Blautia* has been associated also IBS, illustrating that different species within this genus may exert varied effects on the gut ecosystem, potentially influenced by host-specific factors (Rajilić-Stojanović et al., 2011; Liu et al., 2021). Similarly, the increase in *Collinsella* has been linked to low dietary fiber intakes, indicating its adaptability to changes in host dietary patterns (Gomez-Arango et al., 2018). *Weissella* and *Parasutterella* are both recognized as core components of the human gut microbiota (Ju et al., 2019). After one week of washout, *Bifidobacterium* levels increased in both SHIME® lines, hinting at a return to the original status (baseline) after dietary changes (Moreno-Pérez et al., 2018).

5. Conclusions

Although our experiment relies on a single gut ecosystem, and the observations made are simplifications compared to more complex *in vivo* conditions to which gut bacteria are exposed, to the best of our knowledge, this is the first study to explore how plant proteins like RLPI, when pre-fermented, interact at the gut level, providing a middle-term evolution of its bacterial communities. Our findings show that fermentation enhances the nutritional value of pulse proteins by improving protein digestibility, amino acid availability, and the release of bioactive peptides. These changes were associated with a modulation of the gut microbiota toward potentially beneficial profiles, even though temporarily. This work provides important preliminary insights that support further research on the potential of FRLPI as a sustainable, functional ingredient to influence gut microbiota and health.

Data availability

The microbiome raw sequence datasets presented in this study can be found in online repositories. The names of the repository/repositories and accession number(s) are as follows: NCBI BioProject—PRJNA1211871 (<https://www.ncbi.nlm.nih.gov/bioproject/PRJNA1211871/>).

Funding

The work for this publication has been undertaken as part of the SMART PROTEIN project <https://smartproteinproject.eu/objectives/>. This project has received funding from the European Union's Horizon 2020 research and innovation program under grant agreement No. 862957.

Ethical statement

Fecal donor selection and sample resupply for the SHIME system were carefully considered, ensuring that the selected donor was available for resampling when needed. Each volunteer provided written informed consent, and the study protocol was approved by the Research Ethics Committee of the Free University of Bolzano (17 September 2019), in accordance with the Declaration of Helsinki.

CRediT authorship contribution statement

Federica Mastrodonardo: Writing – review & editing, Writing – original draft, Visualization, Validation, Methodology, Investigation. **Stefano Tonini:** Writing – review & editing, Validation, Methodology, Investigation, Formal analysis, Data curation. **Lena GraneHäll:** Visualization, Validation, Software, Formal analysis, Data curation. **Andrea Polo:** Writing – review & editing, Supervision, Methodology. **Emanuele Zannini:** Supervision. **Marco Gobetti:** Funding acquisition, Conceptualization. **Raffaella Di Cagno:** Writing – review & editing, Supervision. **Olga Nikoloudaki:** Writing – review & editing, Writing – original draft, Visualization, Validation, Formal analysis, Data curation, Conceptualization.

Declaration of competing interest

The authors declare that they have no known competing financial interests or personal relationships that could have appeared to influence the work reported in this paper.

Acknowledgements

This work was partially supported by the Open Access funding provided by the Free University of Bozen-Bolzano, Italy.

Supplementary materials

Supplementary material associated with this article can be found, in the online version, at [doi:10.1016/j.fufo.2025.100772](https://doi.org/10.1016/j.fufo.2025.100772).

References

- Aghababaei, F., McClements, D.J., Pignitter, M., Hadidi, M., 2024. A comprehensive review of processing, functionality, and potential applications of lentil proteins in the food industry. *Adv. Colloid. Interface Sci.* 333, 103280. <https://doi.org/10.1016/j.cis.2024.103280>.
- Aiking, H., de Boer, J., 2020. The next protein transition. *Trends. Food Sci. Technol.* 105, 515–522. <https://doi.org/10.1016/j.tifs.2018.07.008>.
- Amigo, L., Hernández-Ledesma, B., 2020. Current evidence on the bioavailability of food bioactive peptides. *Molecules* 25 (19), 4479. <https://doi.org/10.3390/molecules25194479>.
- Balandrán-Quintana, R.R., Mendoza-Wilson, A.M., Montfort, G.R.C., Huerta-Ocampo, J.A., 2019. Plant-based proteins: Sustainable source, Processing and Applications, pp. 97–130. <https://doi.org/10.1016/B978-0-12-816695-6.00004-0>.
- Bao, X., Wu, J., 2021. Impact of food-derived bioactive peptides on gut function and health. *Food Res. Int.* 147, 110485. <https://doi.org/10.1016/j.foodres.2021.110485>.
- Blaak, E.E., Canfora, E.E., Theis, S., Frost, G., Groen, A.K., Mithieux, G., Verbeke, K., 2020. Short chain fatty acids in human gut and metabolic health. *Benef. Microbes* 11 (5), 411–455. <https://doi.org/10.3920/BM2020.0057>.
- Badura, J., Medić, M., Wyk, N.V., Krause, B., Semmler, H., Brezina, S., Pretorius, I.S., Rauhut, D., Wallbrunn, C.V., 2023. Synthesis of aroma compounds as a function of different nitrogen sources in fermentations using non-saccharomyces wine yeasts. *Microorganisms* 11. <https://doi.org/10.3390/microorganisms11010014>.
- Boven, L., Akkerman, R., de Vos, P., 2024. Sustainable diets with plant-based proteins require considerations for prevention of proteolytic fermentation. *Crit. Rev. Food Sci. Nutr.* 1–11. <https://doi.org/10.1080/10408398.2024.2352523>.
- Bryant, C.J., 2022. Plant-based animal product alternatives are healthier and more environmentally sustainable than animal products. *Future Foods* 6, 100174. <https://doi.org/10.1016/j.fufo.2022.100174>.
- Callahan, B.J., McMurdie, P.J., Rosen, M.J., Han, A.W., Johnson, A.J.A., Holmes, S.P., 2016. DADA2: high-resolution sample inference from Illumina amplicon data. *Nat. Methods* 13 (7), 581–583. <https://doi.org/10.1038/nmeth.3869>.
- Chai, K.F., Voo, A.Y.H., Chen, W.N., 2020. Bioactive peptides from food fermentation: a comprehensive review of their sources, bioactivities, applications, and future development. *Compr. Rev. Food Sci. Food Saf.* 19 (6), 3825–3885. <https://doi.org/10.1111/1541-4337.12651>.
- Ciani, M., Comitini, F., 2019. Use of non-Saccharomyces yeasts in red winemaking. *Red Wine Technol.* 51–68. <https://doi.org/10.1016/B978-0-12-814399-5.00004-9>.
- Comitini, F., Agabati, A., Canonico, L., Ciani, M., 2021. Yeast interactions and molecular mechanisms in wine fermentation: a comprehensive review. *Int. J. Mol. Sci.* 22. <https://doi.org/10.3390/ijms22147754>.
- Da Ros, A., Polo, A., Rizzello, C.G., Acin-Albiac, M., Montemurro, M., Di Cagno, R., Gobbetti, M., 2021. Feeding with sustainably sourdough bread has the potential to promote the healthy microbiota metabolism at the colon level. *Microbiol. Spectr.* 9 (3), e00494. <https://doi.org/10.1128/Spectrum.00494-21>.
- De Boer, J., Aiking, H., 2011. On the merits of plant-based proteins for global food security: marrying macro and micro perspectives. *Ecol. Econ.* 70 (7), 1259–1265. <https://doi.org/10.1016/j.ecolecon.2011.03.001>.
- Dhull, S.B., Kinabo, J., Uebbersax, M.A., 2023. Nutrient profile and effect of processing methods on the composition and functional properties of lentils (Lens culinaris Medik): a review. *Legume Sci.* 5 (1), e156. <https://doi.org/10.1002/leg3.156>.
- Di Cagno, R., Filannino, P., Cavoski, I., Lanera, A., Mamdouh, B.M., Gobbetti, M., 2017. Bioprocessing technology to exploit organic palm date (Phoenix dactylifera L. cultivar Siwi) fruit as a functional dietary supplement. *J. Funct. Foods* 31, 9–19. <https://doi.org/10.1016/j.jff.2017.01.033>.
- Diether, N.E., Willing, B.P., 2019. Microbial fermentation of dietary protein: an important factor in diet-microbe-host interaction. *Microorganisms* 7. <https://doi.org/10.3390/microorganisms7010019>.
- Du, H., Lin, Y., Stanton, C., Danilowski, D., Zannini, E., Ross, R.P., Miao, S., 2023. Characterization and functional properties of pH- and heated time-induced aggregates from red lentil protein. *Food Struct.* 37, 100342. <https://doi.org/10.1016/j.foostr.2023.100342>.
- Fassarella, M., Blaak, E.E., Penders, J., Nauta, A., Smidt, H., Zoetendal, E.G., 2021. Gut microbiome stability and resilience: elucidating the response to perturbations in order to modulate gut health. *Gut* 70 (3), 595–605. <https://doi.org/10.1136/gutjnl-2020-321747>.
- Fung, K.Y., Cosgrove, L., Lockett, T., Head, R., Topping, D.L., 2012. A review of the potential mechanisms for the lowering of colorectal oncogenesis by butyrate. *Br. J. Nutr.* 108 (5), 820–831. <https://doi.org/10.1017/S0007114512001948>.
- García-González, N., Battista, N., Prete, R., Corsetti, A., 2021. Health-promoting role of Lactiplantibacillus plantarum isolated from fermented foods. *Microorganisms* 9 (2), 349. <https://doi.org/10.3390/microorganisms9020349>.
- Gomez-Arango, L.F., Barrett, H.L., Wilkinson, S.A., Callaway, L.K., McIntyre, H.D., Morrison, M., Dekker Nitert, M., 2018. Low dietary fiber intake increases Collinsella abundance in the gut microbiota of overweight and obese pregnant women. *Gut. Microbes* 9 (3), 189–201. <https://doi.org/10.1080/19490976.2017.1406584>.
- Grancieri, M., Martino, H.S.D., Gonzalez de Mejia, E., 2019. Chia seed (Salvia hispanica L.) as a source of proteins and bioactive peptides with health benefits: a review. *Compr. Rev. Food Sci. Food Saf.* 18 (2), 480–499. <https://doi.org/10.1111/1541-4337.12423>.
- Gilbert, M.S., Jssennagger, N., Kies, A.K., van Mil, S.W.C., 2018. Protein fermentation in the gut; implications for intestinal dysfunction in humans, pigs, and poultry. *Am. J. Physiol.-Gastrointest. Liver Physiol.* 315, G159–G170. <https://doi.org/10.1152/ajpgi.00319.2017>.
- Guo, Z., Yi, D., Hu, B., Shi, Y., Xin, Y., Gu, Z., Zhang, L., 2021. The alteration of gut microbiota by bioactive peptides: a review. *Syst. Microbiol. Biomanufacturing* 1 (4), 363–377. <https://doi.org/10.1007/s43393-021-00035-x>.
- Hall, A.E., Moraru, C.I., 2021. Effect of high pressure processing and heat treatment on in vitro digestibility and trypsin inhibitor activity in lentil and faba bean protein concentrates. *LWT* 152, 112342. <https://doi.org/10.1016/j.lwt.2021.112342>.
- Hedington, M.S., Davis, S.N., 2019. Considerations when using alpha-glucosidase inhibitors in the treatment of type 2 diabetes. *Expert. Opin. Pharmacother* 20 (18), 2229–2235. <https://doi.org/10.1080/14656566.2019.1672660>.
- Herlemann, D.P., Labrenz, M., Jürgens, K., Bertilsson, S., Wanek, J.J., Andersson, A.F., 2011. Transitions in bacterial communities along the 2000 km salinity gradient of the Baltic Sea. *ISME J.* 5 (10), 1571–1579. <https://doi.org/10.1038/ismej.2011.41>.
- Jeyakumar, E., Lawrence, R., 2022. Microbial fermentation for reduction of antinutritional factors. *Current Developments in Biotechnology and Bioengineering*. Elsevier, pp. 239–260. <https://doi.org/10.1016/B978-0-12-823506-5.00012-6>.
- Joehne, M.S., Jeske, S., Ispiryan, L., Zannini, E., Arendt, E.K., Bez, J., Petersen, I.L., 2021. Nutritional and anti-nutritional properties of lentil (Lens culinaris) protein isolates prepared by pilot-scale processing. *Food Chem.* 9, 100112. <https://doi.org/10.1016/j.fochx.2020.100112>.
- Ju, T., Kong, J.Y., Stothard, P., Willing, B.P., 2019. Defining the role of Parasutterella, a previously uncharacterized member of the core gut microbiota. *ISME J.* 13 (6), 1520–1534. <https://doi.org/10.1038/s41396-019-0364-5>.
- Keller, J., 2013. Gastrointestinal Digestion and Absorption. In: Lennarz, W.J., Lane, M.D. (Eds.), *Encyclopedia of Biological Chemistry*, 2nd Edition. Academic Press, Waltham, pp. 354–359. <https://doi.org/10.1016/B978-0-12-378630-2.00106-7>.
- Kemsawad, V., Viana, T., Ardo, Y., Arneborg, N., 2015. Influence of nitrogen sources on growth and fermentation performance of different wine yeast species during alcoholic fermentation. *Appl. Microbiol. Biotechnol.* 99, 10191–10207. <https://doi.org/10.1007/s00253-015-6835-3>.
- Koiraal, P., Costantini, A., Maina, H.N., Rizzello, C.G., Verni, M., Beni, V.D., Coda, R., 2022. Fermented brewers' spent grain containing dextran and oligosaccharides as ingredient for composite wheat bread and its impact on gut metabolism in vitro. *Fermentation* 8 (10), 487. <https://doi.org/10.3390/fermentation8100487>.
- Kuesten, C., Hu, C., 2020. Functional foods and protein supplementation. *Handbook of Eating and drinking: Interdisciplinary perspectives*, pp. 941–964. https://doi.org/10.1007/978-3-030-14504-0_175.
- Lee, H.W., Lu, Y., Zhang, Y., Fu, C., Huang, D., 2021. Physicochemical and functional properties of red lentil protein isolates from three origins at different pH. *Food Chem.* 358, 129749. <https://doi.org/10.1016/j.foodchem.2021.129749>.
- Liu, X., Mao, B., Gu, J., Wu, J., Cui, S., Wang, G., Chen, W., 2021. Blautia—A new functional genus with potential probiotic properties? *Gut. Microbes* 13 (1), 1875796. <https://doi.org/10.1080/19490976.2021.1875796>.
- Liu, Y., Zhu, S., Li, Y., Sun, F., Huang, D., Chen, X., 2023. Alterations in the multilevel structures of chickpea protein during fermentation and their relationship with digestibility. *Food Res. Int.* 165, 112453. <https://doi.org/10.1016/j.foodres.2022.112453>.
- Lleixà, J., Martín, V., Giorello, F., Portillo, M.C., Carrau, F., Beltran, G., Mas, A., 2019. Analysis of the NCR mechanisms in hanseniaspora vineae and saccharomyces cerevisiae during winemaking. *Front. Genet.* 9-2018.
- Lotti, C., Rubert, J., Fava, F., Tuohy, K., Mattivi, F., Vrhovsek, U., 2017. Development of a fast and cost-effective gas chromatography-mass spectrometry method for the quantification of short-chain and medium-chain fatty acids in human biofluids. *Anal. Bioanal. Chem.* 409, 5555–5567. <https://doi.org/10.1007/s00216-017-0493-5>.
- Louis, P., Flint, H.J., 2017. Formation of propionate and butyrate by the human colonic microbiota. *Environ. Microbiol.* 19 (1), 29–41. <https://doi.org/10.1111/1462-2920.13589>.
- Lozupone, C.A., Stombaugh, J.I., Gordon, J.I., Jansson, J.K., Knight, R., 2012. Diversity, stability and resilience of the human gut microbiota. *Nature* 489 (7415), 220–230. <https://doi.org/10.1038/nature11550>.
- Lumsden, C.L., Jägermeyr, J., Ziska, L., Fanzo, J., 2024. Critical overview of the implications of a global protein transition in the face of climate change: key unknowns and research imperatives. *One Earth* 7 (7), 1187–1201. <https://doi.org/10.1016/j.oneear.2024.06.013>.
- Macfarlane, G.T., Allison, C., 1986. Utilisation of protein by human gut bacteria. *FEMS Microbiol. Ecol.* 2 (1), 19–24. <https://doi.org/10.1111/j.1574-6968.1986.tb01934.x>.

- Mallick, H., Rahnavard, A., McIver, L.J., Ma, S., Zhang, Y., Nguyen, L.H., Huttenhower, C., 2021. Multivariable association discovery in population-scale meta-omics studies. *PLoS Comput. Biol.* 17 (11), e1009442. <https://doi.org/10.1371/journal.pcbi.1009442>.
- Martin-Gallausiaux, C., Marinelli, L., Blottière, H.M., Larraufie, P., Lapaque, N., 2021. SCFA: mechanisms and functional importance in the gut. *Proc. Nutr. Soc.* 80 (1), 37–49. <https://doi.org/10.1017/S0029665120006916>.
- Martini, S., Conte, A., Tagliazucchi, D., 2020. Effect of ripening and in vitro digestion on the evolution and fate of bioactive peptides in Parmigiano-Reggiano cheese. *Int. Dairy J.* 105, 104668. <https://doi.org/10.1016/j.idairyj.2020.104668>.
- Minkiewicz, P., Iwaniak, A., Darewicz, M., 2019. BIOPEP-UWM database of bioactive peptides: current opportunities. *Int. J. Mol. Sci.* 20 (23), 5978. <https://doi.org/10.3390/ijms20235978>.
- Minnebo, Y., Delbaere, K., Goethals, V., Raes, J., Van de Wiele, T., De Paepe, K., 2023. Gut microbiota response to in vitro transit time variation is mediated by microbial growth rates, nutrient use efficiency and adaptation to in vivo transit time. *Microbiome* 11 (1), 240. <https://doi.org/10.1186/s40168-023-01691-y>.
- Molly, K., Vande Woestyne, M., Verstraete, W., 1993. Development of a 5-step multi-chamber reactor as a simulation of the human intestinal microbial ecosystem. *Appl. Microbiol. Biotechnol.* 39, 254–258. <https://doi.org/10.1007/BF00228615>.
- Moreno-Pérez, D., Bressa, C., Bailén, M., Hamed-Bousdar, S., Naclerio, F., Carmona, M., Larrosa, M., 2018. Effect of a protein supplement on the gut microbiota of endurance athletes: a randomized, controlled, double-blind pilot study. *Nutrients* 10 (3), 337. <https://doi.org/10.3390/nu10030337>.
- Neis, E.P.J.G., Dejong, C.H.C., Rensen, S.S., 2015. The role of microbial amino acid metabolism in host metabolism. *Nutrients* 7, 2930–2946. <https://doi.org/10.3390/nu7042930>.
- Nosworthy, M.G., Franczyk, A.J., Medina, G., Neufeld, J., Appah, P., Utioh, A., Frohlich, P., House, J.D., 2017. Effect of processing on the in vitro and in vivo protein quality of yellow and green split peas (*Pisum sativum*). *J. Agric. Food Chem.* 65, 7790–7796. <https://doi.org/10.1021/acs.jafc.7b03597>.
- Nosworthy, M.G., Medina, G., Lu, Z.-H., House, J.D., 2023. Plant proteins: methods of quality assessment and the human health benefits of pulses. *Foods* 12. <https://doi.org/10.3390/foods12152816>.
- Ngo, N.T.T., Senadheera, T.R., Shahidi, F., 2023. Antioxidant properties and prediction of bioactive peptides produced from flaxseed (*sophia*, *Descurainis sophia* L.) and Camelina (*Camelina sativa* (L.) Crantz) Seed Meal: integrated in vitro and in silico studies. *Plants* 12 (20), 3575. <https://doi.org/10.3390/plants12203575>.
- Onetto, C.A., McCarthy, J., Schmidt, S.A., 2025. A rapid growth rate underpins the dominance of *hanseniaspora uvarum* in spontaneous grape juice fermentations. *Yeast*. <https://doi.org/10.1002/yea.4000> n/a.
- Ozato, N., Saito, S., Yamaguchi, T., Katashima, M., Tokuda, I., Sawada, K., Nakaji, S., 2019. *Blautia* genus associated with visceral fat accumulation in adults 20–76 years of age. *NPJ. Biofilms. Microbiomes* 5 (1), 28. <https://doi.org/10.1038/s41522-019-0101-x>.
- Palomino, M.M., Allievi, M.C., Gordillo, T.B., Bockor, S.S., Fina Martin, J., Ruzal, S.M., 2023. Surface layer proteins in species of the family *Lactobacillaceae*. *Microb. Biotechnol.* 16 (6), 1232–1249. <https://doi.org/10.1111/1751-7915.14230>.
- Paoletti, A., Courtney-Martin, G., Elango, R., 2024. Determining amino acid requirements in humans. *Front. Nutr.* 11–2024.
- Sun, Q., An, P., Li, P., Wang, H., Tao, S., Liu, Y., 2025. Unraveling time-resolved transcriptional and metabolic shifts in the mixed fermentation of *saccharomyces cerevisiae* and *hanseniaspora uvarum*. *J. Agric. Food Chem.* 73, 12418–12432. <https://doi.org/10.1021/acs.jafc.5c00722>.
- Pang, Z., Lu, Y., Zhou, G., Hui, F., Xu, L., Viau, C., Xia, J., 2024. MetaboAnalyst 6.0: towards a unified platform for metabolomics data processing, analysis and interpretation. *Nucleic. Acids. Res.* 253. <https://doi.org/10.1093/nar/gkae253>.
- Polo, A., Albiac, M.A., Da Ros, A., Ardévol, V.N., Nikoloudaki, O., Verté, F., Gobetti, M., 2023. The effect of hydrolyzed and fermented arabinoxylan-oligo saccharides (AXOS) intake on the middle-term gut microbiome modulation and its metabolic answer. *Nutrients* 15 (3), 590. <https://doi.org/10.3390/nu15030590>.
- Qin, W., Xia, Y., Xiong, Z., Song, X., Ai, L., Wang, G., 2022. The intestinal colonization of *Lactiplantibacillus plantarum* AR113 is influenced by its mucins and intestinal environment. *Food Res. Int.* 157, 111382. <https://doi.org/10.1016/j.foodres.2022.111382>.
- Rajilić-Stojanović, M., Biagi, E., Heilig, H.G., Kajander, K., Kekkonen, R.A., Tims, S., de Vos, W.M., 2011. Global and deep molecular analysis of microbiota signatures in fecal samples from patients with irritable bowel syndrome. *Gastroenterology* 141 (5), 1792–1801. <https://doi.org/10.1053/j.gastro.2011.07.043>.
- Rinninella, E., Raoul, P., Cintoni, M., Franceschi, F., Miggiaro, G.A.D., Gasbarrini, A., Mele, M.C., 2019. What is the healthy gut microbiota composition? A changing ecosystem across age, environment, diet, and diseases. *Microorganisms* 7 (1), 14. <https://doi.org/10.3390/microorganisms7010014>.
- Roy, F., Boye, J.I., Simpson, B.K., 2010. Bioactive proteins and peptides in pulse crops: pea, chickpea and lentil. *Food Res. Int.* 43 (2), 432–442. <https://doi.org/10.1016/j.foodres.2009.09.002>.
- Sá, A.G., Hang, J., Jardine, L., Bett, K.E., House, J.D., 2023. How different amino acid scoring patterns recommended by FAO/WHO can affect the nutritional quality and protein claims of lentils. *Sustain. Food Proteins* 1 (2), 59–73. <https://doi.org/10.1002/sfp2.1008>.
- Sánchez, A., Vázquez, A., 2017. Bioactive peptides: a review. *Food Qual. Saf.* 1 (1), 29–46. <https://doi.org/10.1093/fqsaf/fyx006>.
- Tlais, A.Z.A., Kanwal, S., Filannino, P., Albiac, M.A., Gobetti, M., Di Cagno, R., 2022. Effect of sequential or ternary starters-assisted fermentation on the phenolic and glucosinolate profiles of sauerkraut in comparison with spontaneous fermentation. *Food Res. Int.* 156, 111116. <https://doi.org/10.1016/j.foodres.2022.111116>.
- Tonini, S., Tlais, A.Z.A., Galli, B.D., Helal, A., Tagliazucchi, D., Filannino, P., Di Cagno, R., 2024. Lentils protein isolate as a fermenting substrate for the production of bioactive peptides by lactic acid bacteria and neglected yeast species. *Microb. Biotechnol.* 17 (1), e14387. <https://doi.org/10.1111/1751-7915.14387>.
- Van de Wiele, T., Van den Abbeele, P., Ossieur, W., Possemiers, S., & Marzorati, M., 2015. The simulator of the human intestinal microbial ecosystem (SHIME®). The Impact of Food Bioactives on Health: in vitro and ex vivo models, 305–317. https://doi.org/10.1007/978-3-319-16104-4_27.
- Walker, A.W., Ince, J., Duncan, S.H., Webster, L.M., Holtrop, G., Ze, X., Flint, H.J., 2011. Dominant and diet-responsive groups of bacteria within the human colonic microbiota. *ISME J.* 5 (2), 220–230. <https://doi.org/10.1038/ismej.2010.118>.
- Walter, J., O'Toole, P.W., 2023. Microbe profile: the *Lactobacillaceae*. *Microbiology* 169 (12), 001414. <https://doi.org/10.1099/mic.0.001414>.
- Wu, J., Liao, W., Udenigwe, C.C., 2017. Revisiting the mechanisms of ACE inhibitory peptides from food proteins. *Trends. Food Sci. Technol.* 69, 214–219. <https://doi.org/10.1016/j.tifs.2017.07.011>.
- Yao, S., Zhao, Y., Chen, H., Sun, R., Chen, L., Huang, J., Chen, S., 2023. Exploring the plasticity of diet on gut microbiota and its correlation with gut health. *Nutrients* 15 (15), 3460.
- Zafar, H., Saier Jr, M.H., 2021. Gut *Bacteroides* species in health and disease. *Gut. Microbes* 13 (1), 1848158. <https://doi.org/10.3390/nu15153460>.
- Zhu, Y., Lao, F., Pan, X., Wu, J., 2022. Food protein-derived antioxidant peptides: molecular mechanism, stability and bioavailability. *Biomolecules* 12 (11), 1622. <https://doi.org/10.3390/biom12111622>.